Chemistry & Biology, Vol. 11, 1301–1306, September, 2004, ©2004 Elsevier Ltd. All rights reserved. DOI 10.1016/j.chembiol.2004.07.009

Discovery of Picomolar Slow Tight-Binding Inhibitors of α-Fucosidase

Chuan-Fa Chang,[1,3] Chin-Wen Ho,[1,3] Chung-Yi Wu,[1] Tsrong-An Chao,[1] Chi-Huey Wong,[1,2] and Chun-Hung Lin[1,*]

[1]The Genomic Research Center and Institute of Biological Chemistry
Academia Sinica
No. 128 Academia Road Section 2
Nan-Kang, Taipei 11529
Taiwan

[2]Department of Chemistry and the Skaggs Institute for Chemical Biology
The Scripps Research Institute
10550 North Torrey Pines Road
La Jolla, California 92037

Summary

Glycosidase inhibitors have shown great medicinal and pharmaceutical values as exemplified by the therapeutic treatment of influenza virus and non-insulin-dependent diabetes. We herein report the discovery of picomolar slow tight-binding inhibitors 2–5 against the α-fucosidase from *Corynebacterium sp.* by a rapid screening for an optimal aglycon attached to 1-aminomethyl fuconojirimycin (1). The time-dependent inhibition displays the progressive tightening of enzyme-inhibitor complex from a low nanomolar K_i to picomolar K_i* value. Particularly compound 2 with a K_i* of 0.46 pM represents the most potent glycosidase inhibitor to date. The effect of compound 3 on the intrinsic fluorescence of α-fucosidase is both time- and concentration-dependent in a saturation-type manner, which is consistent with the initial formation of a rapid equilibrium complex of enzyme and inhibitor (E•I), followed by the slower formation of a tightly bound enzyme-inhibitor complex (E•I*). The binding affinity increases 3.5 × 10^4-fold from 1 (K_i = 16.3 nM) to 2 (K_i* = 0.46 pM). This work clearly demonstrates the effectiveness of our combinatorial approach leading to the rapid discovery of potent inhibitors.

Introduction

Glycosidases catalyze the cleavage of glycosidic bonds associated with important biological activities, including metabolic disorders [1, 2], viral and bacterial infection [3], tumor occurrence/metastasis [4, 5], glycoprotein folding [6, 7] and function [8], and many other intercellular recognition processes. Some of these enzymes have been considered as important targets for therapeutic development. The neuraminidase inhibitor Tamiflu or oseltamivir phosphate, for example, has been prescribed to treat the infection of influenza virus [9]. *N*-hydroxyethyldeoxynojirimycin (namely Glyset or Miglitol), targeting the intestinal disaccharidases [10], has been commercially available since 1996 for the treatment of type II diabetes [1, 2]. As a consequence, the development of potent glycosidase inhibitors has been shown extensive interest in the past decade.

Among members of the glycosidase family, α-fucosidase is involved in the removal of nonreducing terminal L-fucose residues that are connected to oligosaccharides via α1,2-; α1,3-; α1,4-; or α1,6-linkages. Owing to a great variety of physiological and pathological events associated with fucose-containing glycoconjugates [11–13], increasing attention has been drawn to certain specific α-fucosidases [14, 15]. For instance, an aberrant distribution of α-fucosidase has been reported relevant to inflammation [16], cancer [17, 18], and cystic fibrosis [19, 20]. These enzymes have been recognized as diagnostic markers for the early detection of colorectal and hepatocellular cancers because of the presence of α-fucosidase in these patients' sera [17, 18, 21]. On the other hand, potent α-fucosidase inhibitors may be used to study their functions and develop potential therapeutic agents.

We have recently developed a rapid generation of libraries of compounds in microplates for high throughput screening in situ without protecting group manipulation and product isolation, and have identified the most potent and selective inhibitors against the α-fucosidase from bovine kidney as well as *Corynebacterium sp*. [22]. This strategy is based on a rapid screening for an optimal aglycon attached to the fuconojirimycin (FNJ)-based structure that mimics the transition state of enzymatic glycoside cleavage. The library screened for two α-fucosidases generated different groups of structures, indicating that our approach is effective and simple for identification of potent inhibitors that are enzyme specific [22], and have little or no inhibition activity against other glycosidase members (e.g., glucosidase, galactosidase, and mannosidase) [22]. We report the discovery of slow and tight binding inhibitors of α-fucosidase using this approach. The introduction of a hydrophobic moiety to the iminocyclitol core not only resulted in the time-dependent inhibition, but also greatly enhanced the inhibitory potency to give the K_i* value in the pM range.

Results and Discussion

1-aminomethyl FNJ (**1**, Figure 1) [22] was used for diversity-oriented reaction with various acids in the presence of (1*H*-benzotrizole-1-yl)-1,1,3,3-tetramethyluronium hexafluoorophosphate (HBTU, 1 equiv) and diisopropyl ethylamine (DIEA, 2 equiv) in DMF, followed by aqueous dilution and screening without purification [22], as shown in Figure 2. Several molecules were identified as potent and competitive inhibitors against the α-fucosidase from *Corynebacterium sp*. with the IC_{50} values in the low nM range. The screening was based on the detection of fluorescence emission of 4-methylumbelliferone at 465 nm in the presence of 4-methylumbelliferyl-α-L-fucopyranoside (or *p*-nitrophenol at 405 nm in the presence of

*Correspondence: chunhung@gate.sinica.edu.tw
[3]These authors contributed equally to this work.

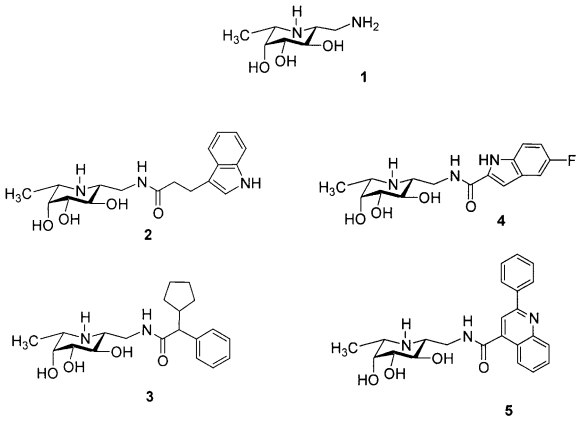

Figure 1. Structures of Compounds **1–5**

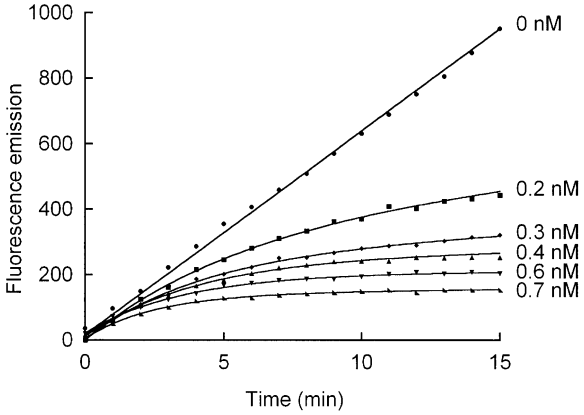

Figure 3. Time-Dependent Inhibition of α-Fucosidase by Compound **2**

p-nitrophenyl-α-L-fucopyranoside) [22]. It was observed during the prolonged observation of enzyme inhibition assay that there was a time-dependent decrease in the reaction rate as a function of the inhibitor concentration. Interestingly, nearly all the members of the library exhibited, more or less, time-dependent slow tight-binding inhibition (e.g., the inhibition of compound **2**, see Figure 3). In a sharp contrast to the amide-forming reaction products, compound **1** is a reversible inhibitor with K_i value of 16.3 nM (Figure 4).

In order to investigate the inhibition mechanism, four FNJ derivatives (**2–5**) with different aglycon structures and inhibitory potency were individually prepared and purified. Analysis of the progress curves follows the pattern in which an initial collisional complex (E·I) isomerizes to a tighter complex (E·I*) according to equation 1, where E stands for free enzyme, I is free inhibitor, E·I is a rapidly forming preequilibrium complex, and E·I* is the final enzyme-inhibitor complex [23, 24]. All the inhibitors were found to produce progressive tightening of inhibition in a two-step manner, which was corroborated by the fact that the inhibitor has a measurable effect on the initial rates before the onset of slow tight-binding inhibition. Further examination of the progress curves exhibited a time range where the initial rate of reaction did not deviate from linearity.

$$E + I \underset{k_4}{\overset{k_3}{\rightleftharpoons}} E{\cdot}I \underset{k_6}{\overset{k_5}{\rightleftharpoons}} E{\cdot}I^* \qquad (1)$$

K_i, ΔG_1

K_i^*, ΔG_2

Fitting the measured data to this model allowed determination of K_i, $K_i^*$and other numbers (Table 1, see equations 2–5 for the details in the Experimental Procedures). To access the reversibility of the enzyme-inhibitor complex, the α-fucosidase was preincubated with each individual inhibitor (**2–5**) for 60 min at 20°C to fully inactivate the enzyme. Then, an excessive 10^5-fold dilution was made into a reaction mixture containing 100 μM 4-methylumbelliferyl-α-L-fucopyranoside to monitor the recovery of activity (Figure 5). The result determined the rate constant of k_6 (rate of regain of activity from fully inhibited state) and corresponding $t_{1/2}$ (half-life of E·I*), as shown in Table 1.

In distinction from compound **1**, all the coupling products **2–5** displayed time-dependent progressive inhibition with a 696-, 225-, 23-, and 29-fold tightening (i.e., the values of K_i/K_i^* in Table 1), respectively, from low nanomolar K_i to picomolar K_i^* values. Especially compound **2**, superior to others in the α-fucosidase inhibition with a K_i^* of 0.46 pM, represents the most powerful glycosidase inhibitor yet described. As a consequence, our rapid diversity-based synthesis and subsequent in situ screening is able to promptly identify an optimal hydrophobic group for enhancement of the inhibition up to 3.5 × 10^4-fold, when comparing the binding affinity of **1** (K_i = 16.3 nM) and **2** (K_i^* = 0.46 pM). The resulting feature of slow-dissociating enzyme-inhibitor complex is pharmacologically useful as exemplified by the β-lactamase inhibitors sulbactam and olivanate [25], and the antihypertensive drug against angiotensin-converting enzyme [26, 27].

The kinetic analysis of α-fucosidase inhibition revealed a two-step inhibition mechanism. To study whether this isomerization is related to the conformational change in α-fucosidase due to binding of the inhibitor, the fluores-

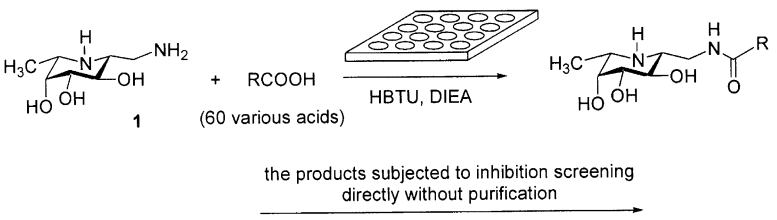

Figure 2. Rapid Diversity-Oriented Synthesis in Microtiter Plates Followed by High-Throughput Screening In Situ without Product Purification

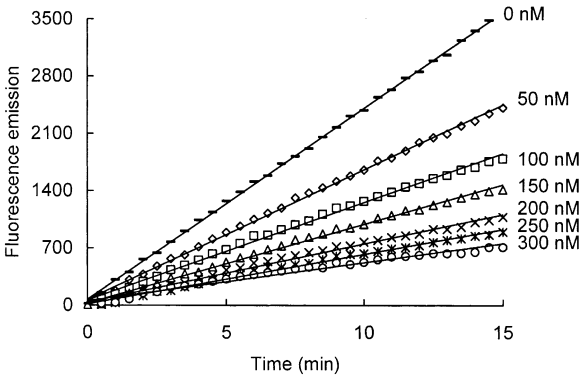

Figure 4. Progress Curves for the Inhibition of α-Fucosidase by 1-Aminomethyl FNJ (**1**)

The figure shows that compound **1** is a reversible inhibitor.

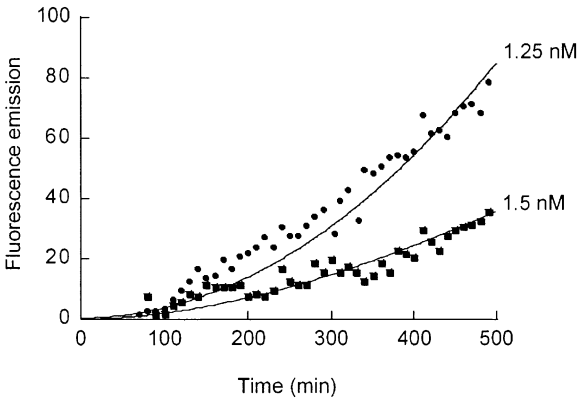

Figure 5. Determination of the Dissociation Rate Constant and Half-Life for Regain of Catalytic Activity

The α-fucosidase was preincubated with different concentrations of compound **2** at 20°C for 60 min. An aliquot was then removed, diluted 10^5-fold, and assayed for the recovery of the enzyme activity.

cence emission spectra of α-fucosidase was analyzed in the presence and absence of the inhibitor (**3**). The enzyme exhibited an emission maxima (λ_{max}) at 336 nm as a consequence of the radiative enhancement of π–π^* transition from the tryptophan residues, as shown in Figure 6A. The binding of compound **3** resulted in a concentration-dependent increase of the fluorescence. Titration of inhibitor **3** against the α-fucosidase demonstrated that the magnitude of the initial rapid fluorescence increase ($F-F_0$) rose hyperbolically, which agreed well with the two-phase, slow tight inhibition (Figure 6B) [28–30]. Furthermore, the effect of the inhibitor **3** on the α-fucosidase was also time dependent in a saturation-type manner, displaying an exponential increase and subsequent slow increase in fluorescence intensity. The values of the derived first-order rate constants (k_{obs}) at each inhibitor concentration gave values of K_i and k_5 of 1.17 nM and 0.057 s^{-1}, respectively (see Experimental Procedures for the details). These numbers are comparable to those obtained from the previously mentioned kinetic analysis. Therefore, the consistency clearly links the observed intrinsic protein fluorescence changes with inhibitor binding.

According to the literature, the slow binding or slow-onset inhibition is prevalent among potent glycosidase inhibitors, in particular iminocyclitols and certain indolizine alkaloids [23, 31]. The phenomenon was attributed to the slow interchange between protein conformations. Nevertheless, the previous studies by Bols et al. indicated that 1-azafagomin and hydrazine-containing analogs are also slow binding inhibitors [32]. Such time-dependent inhibition was demonstrated as a consequence of relatively slow dissociation and association of the inhibitor from and with the enzyme [32]. The binding was contributed by very large positive entropy, which is very different from the thermodynamics of 1-deoxynojirimycin [33]. On the other hand, the analysis of our inhibitors was consistent with the two-step inhibition mechanism, where the E·I complex isomerizes to a tightly bound, slow-dissociating E·I* complex. This conformational change induced in the α-fucosidase was supported by the measurement of intrinsic protein fluorescence.

In addition, Schramm et al. have established extensive investigations of purine nucleoside phosphorylase (PNP) inhibitors [34]. In their reports, immucillin-H and analogs are also slow-onset, tight-binding inhibitors [35]. The crystal structure of PNP supports shorter distances of H-bonds in the enzyme-inhibitor complex than in the Michaelis complex of enzyme-substrate, to be the cause of the observed high affinity [34, 36]. The enhanced inhibitory potency in our study is possibly due to the additional hydrophobic interaction ($\Delta\Delta G = -16.2$, -13.4, -7.8, and -8.3 kJ/mol of compounds **2–5**, respectively) to bring closer the enzyme-inhibitor complex via localized conformational change. The interpretation seems to agree well with our observation that almost

Table 1. Inhibition Constants of Compounds **1–5** against the α-Fucosidase from *Corynebacterium sp*.

	1	**2**	**3**	**4**	**5**
K_i (nM)	16.3 ± 2.5	0.32 ± 0.02	1.24 ± 0.23	1.15 ± 0.18	1.37 ± 0.33
K_i^* (pM)	—	0.46 ± 0.03	5.5 ± 0.2	49 ± 5	47 ± 6
K_i/K_i^*	—	696	225	23	29
k_5 (s^{-1})	—	2.7×10^{-1}	7.2×10^{-2}	5.1×10^{-2}	9.9×10^{-2}
k_6 (s^{-1})	—	3.9×10^{-4}	3.2×10^{-4}	2.1×10^{-3}	3.3×10^{-3}
$t_{1/2}$ (min)	—	30	36	5.5	3.5
ΔG_1 (kJ/mol)[a]	−44.4	−54.2	−50.8	−51.0	−50.6
ΔG_2 (kJ/mol)[b]	—	−70.4	−64.2	−58.8	−58.9

[a] Free energy change to give E·I complex (see Equation 1).
[b] Free energy change to give E·I* complex (see Equation 1).

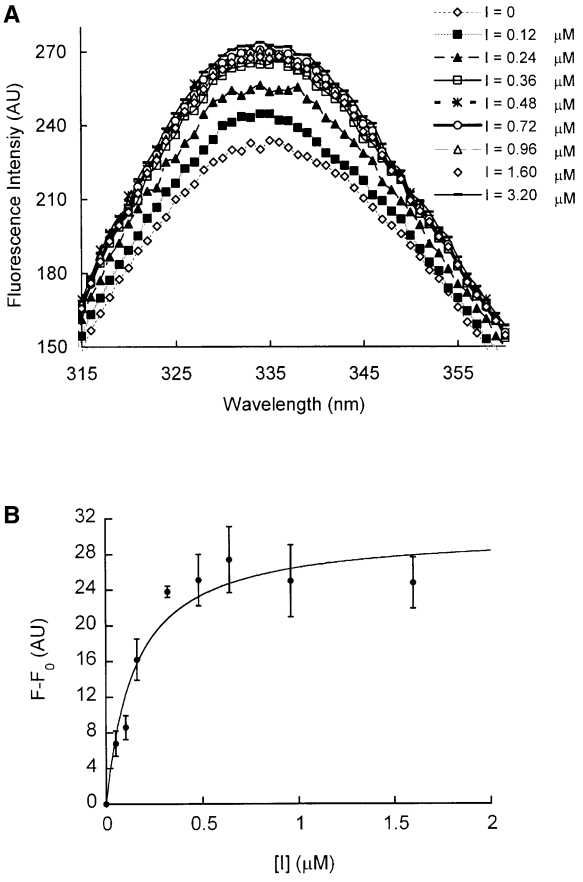

Figure 6. Fluorescence Emission Spectra and Effect of Concentration

(A) Steady-state fluorescence emission spectra of α-fucosidase as a function of compound 3.

(B) Effect of compound 3 concentration on the tryptophanyl fluorescence of α-fucosidase.

all the amide-forming reaction products in Figure 2 (the coupling reaction of **1** with various acids) were slow tight-binding inhibitors, i.e., a hydrophobic domain near the active site may exist to facilitate such interaction. Interestingly, the same library of FNJ derivatives in Figure 2 shows only reversible inhibition against the bovine kidney α-fucosidase, implying a different structural arrangement surrounding the enzyme active site. (Recently, Bourne and Henrissat et al. reported the structural determination of *Thermotoga maritima* α-fucosidase [14] More insight can be revealed from the sequence alignment among different species as well as the molecular modeling.) Our observation seems to be consistent with the report from Ganem and coworkers that very similar enzymes can be distinguished by the introduction of a charge or hydrophobic feature to inhibitors [37, 38].

Significance

A simple and efficient approach has been developed for quick identification and optimization of α-fucosidase inhibitors, including slow tight-binding inhibitors. The study demonstrates that an additional high-affinity binding component, especially the one with hydrophobic nature, connected to a transition-state mimic, can be rapidly identified. The slow and tight binding behavior observed in this study may be caused by the hydrophobic group to induce conformational change to further augment the inhibitory potency. As a consequence, with the incorporation of an optimized aglycon to 1-aminomethyl FNJ (1, K_i = 16.3 nM), the resulting inhibitor 2 is the most potent glycosidase inhibitor with a K_i* of 0.46 pM. Work is in progress to determine the structure of the enzyme-inhibitor complex to further understand the mechanism of inhibition. The slow-releasing feature of the inhibition process also provides a new direction in drug design.

Experimental Procedures

Materials and Reagents

Analytical TLC was performed on precoated plates (Merck, silica gel 60F-254). Silica gel used for flash column chromatography was Mallinckrodt Type 60 (230–400 mesh). Reagents of the highest purity were purchased from Aldrich, Sigma, Acros, and Novabiochem.

1β-Aminomethyl FNJ (1)

^{1}H NMR (400 MHZ, D_2O) δ 3.81 (d, J = 2.4 Hz, 1H, H_4), 3.57 (dd, J = 2.4, 9.6 Hz, 1H, H_3), 3.49 (t, J = 9.6 Hz, 1H, H_2), 3.34 (dd, J = 5.3, 13.2 Hz, 1H, CH_2), 3.05 (dd, J = 7.0, 13.2 Hz, 1H, CH_2), 2.90 (q, J = 6.7 Hz, 1H, H_5), 2.79 (ddd, J = 5.3, 7.0, 9.6 Hz, 1H, H_1), 1.12 (d, J = 6.7 Hz, 3H, H_6 (CH_3)). ^{13}C NMR (100 MHZ, D_2O) δ 75.19, 72.63, 71.07, 57.09, 53.13, 41.88, 16.66.

Typical Procedure of Amide-Forming Reaction (Synthesis of Compound 5)

To a solution of a free amine **1** (34 mg, 0.193 mmol) and 2-phenyl-4-quinolinecarboxylic acid (52.9 mg, 0.212 mmol) in 2 ml dry DMF was added HBTU (80.4 mg, 0.212 mmol) and DIEA (73.8 μL, 0.424 mmol) at 25°C under atmospheric pressure of N_2. The reaction mixture was stirred for 30 min and then quenched by addition of brine and extracted with EtOAc. The organic layer was washed with 1 N HCl, saturated aqueous $NaHCO_3$, and brine, dried over $MgSO_4$, filtered, and concentrated in vacuo. The resulting residue was purified by flash chromatography with $CHCl_3$/MeOH (3/1, R_f = 0.37) to give the desired product **5** (69 mg) in 88% yield.

Compound 2

The synthesis was carried out in the same manner as previously described. Yield 90%, $[\alpha]^{25}_D$ = + 6.2 (c 1.0, MeOH). ^{1}H NMR (400 MHZ, MeOH-*d*4) δ 7.49 (d, J = 8.0 Hz, 1H), 7.25 (d, J = 8.0 Hz, 1H), 7.03–6.91 (m, 3H), 3.74 (d, J = 2.8 Hz, 1H, H_4), 3.57 (t, J = 9.6 Hz, 1H, H_2), 3.48–3.44 (m, 1H, $H_{1'}$), 3.39 (dd, J = 9.6 Hz, J = 2.8 Hz, 1H, H_3), 3.24–3.23 (m, 1H, $H_{1'}$), 3.19 (q, J = 6.7 Hz, 1H, H_5), 3.01 (t, J = 7.6 Hz, 2H), 2.84 (ddd, J = 11 Hz, J = 6.2 Hz, J = 2.7 Hz, H_1), 2.56 (t, J = 7.6 Hz, 2H), 1.29 (d, J = 6.7 Hz, 3H). ^{13}C NMR (100 MHZ, MeOH-*d*4) δ 178.37, 138.22, 128.64, 123.28, 122.48, 119.72, 119.39, 114.92, 112.42, 75.18, 71.36, 67.99, 61.47, 59.32, 40.13, 39.01, 22.67, 15.30. ESI-MS: *m/z* 348 (M + 1).

Compound 3 (Diasteromers)

The synthesis was carried out in the same manner as previously mentioned. Yield 89%, ^{1}H NMR (400 MHZ, MeOH-*d*4) δ 7.34–7.15 (m, 10H), 3.65 (d, J = 2.8 Hz, 2H), 3.49–3.25 (m, 8H), 3.15 (d, J = 11.1 Hz, 2H), 2.90–2.81 (m, 2H), 2.62–2.50 (m, 4H), 1.91–0.88 (m, 22H). ^{13}C NMR (100 MHZ, MeOH-*d*4) δ 178.00, 177.88, 141.59, 141.53, 129.57, 129.39, 129.35, 129.33, 128.22, 128.20, 76.72, 76.67, 73.34, 73.18, 70.41, 70.21, 61.26, 61.18, 60.30, 60.27, 55.03, 55.99, 44.36, 44.21, 41.58, 41.49, 32.68, 32.60, 31.92, 31.89, 26.36, 26.33, 26.04, 26.01, 17.32, 17.16. ESI-MS: *m/z* 363 (M + 1).

Compound 4

The synthesis was carried out in the same manner as previously mentioned. Yield 86%, $[\alpha]^{25}_D = +4.8$ (c 1.0, MeOH). ^{1}H NMR (400 MHZ, MeOH-*d*4) δ 7.49–7.03 (m, 4 H), 3.92–3.84 (m, 2H), 3.88 (d, *J* = 2.8 Hz, 1H), 3.82 (t, *J* = 10 Hz, 1H), 3.60 (dd, *J* = 2.8, 9.6 Hz, 1H), 3.47 (q, *J* = 6.6 Hz, 1H), 3.35 (dd, *J* = 1.6, 3.2 Hz, 1H), 3.25 (ddd, *J* = 3.0, 6.2, 10.0 Hz, 1H), 1.44 (d, *J* = 6.7 Hz, 3H). ^{13}C NMR (100 MHZ, MeOH-*d*4) δ 165.7, 160.8, 158.4, 135.3, 114.5, 114.2, 107.0, 106.8, 105.2, 75.3, 71.5, 68.2, 61.7, 56.5, 40.4, 15.3. ESI-MS: *m/z* 338 (M + 1).

Compound 5

$[\alpha]^{25}_D = +1.2$ (c 1.0, MeOH). ^{1}H NMR (400 MHZ, MeOH-*d*4) δ 8.35–7.50 (m, 10 H), 3.99 (dd, *J* = 3.0, 15.0 Hz, 1H), 3.93–3.80 (m, 3H), 3.55 (dd, *J* = 1.8, 9.3 Hz, 1H), 3.44 (q, *J* = 6.7 Hz, 1H), 3.32 (ddd, *J* = 3.0, 6.7, 10.2 Hz, 1H), 3.24 (dd, *J* = 1.5, 3.2 Hz, 1H), 1.36 (d, *J* = 6.7 Hz, 3H). ^{13}C NMR (100 MHZ, MeOH-*d*4) δ 170.6, 158.2, 146.9, 146.1, 137.6, 133.3, 132.3, 130.5, 129.7, 129.5, 127.9, 127.1, 125.2, 119.8, 75.3, 71.5, 68.5, 60.7, 56.6, 40.9, 15.3. ESI-MS: *m/z* 408 (M + 1).

Synthesis and Inhibition Assay of α-Fucosidase In Situ

The synthesis of amide derivatives in microplates was carried out as described previously [22]. Assay mixtures of 200 μl contained 50 mM HEPES (pH 8.0), 0.1% BSA (by weight), 50 μM 4-methylumbelliferyl-α-L-fucopyranoside, and inhibitor (final concentrations: 1.0–3.0 nM). The α-fucosidase (0.2 nM) was added to initiate inhibition assays. The emission at 465 nm was monitored using an excitation wavelength of 360 nm to measure the release of fluorescent 4-methylumbelliferone at 20°C. When 200 μM *p*-nitrophenyl-α-L-fucopyranoside was used as the substrate, the absorption at 405 nm was measured for the release of *p*-nitrophenol.

The resulting data were analyzed and determined to follow the aforementioned slow binding inhibition pattern (equation 1). The kinetics can be described according to an integrated equation (equation 2), in which V_0 and V_S are the initial and the steady-state rates, k is the apparent rate constant for establishing the steady-state equilibrium, and P is amount of product accumulated during a period of time t.

$$P = V_S \cdot t + (V_0 - V_S)\frac{(1 - e^{-kt})}{k} \quad (2)$$

In the case of slow tight-binding inhibition, the concentration of E·I is not negligible in comparison with the inhibitor concentration and the free inhibitor concentration is not equal to the added concentration of the inhibitor. Corrections have to be made for the reductions in the inhibitor concentration that occurs on formation of the E·I complex. The variation of the steady-state velocity with inhibitor concentration is given by the equations

$$V_S = \frac{k_7\,[S]\,Q}{2\,(K_m + [S])} \quad (3)$$

$$Q = \sqrt{(K_i' + [I]_t + [E]_t)^2 + 4\,K_i'\,[E]_t} - (K_i' + [I]_t - [E]_t) \quad (4)$$

where $K_i' = K_i^*\,(1 + [S]/K_m)$, k_7 is the rate constant for the product formation, and $[I]_t$ and $[E]_t$ stand for total inhibitor and enzyme concentrations, respectively. The relationship between the rate constant of enzymatic reaction *k* and the interconversion of E·I and E·I* can be expressed as equation 5.

$$k = k_6 + k_5\left[\frac{[I]/K_i}{1 + ([S]/K_m) + ([I]/K_i)}\right] \quad (5)$$

The progress curves were analyzed by equations 2 and 5 using nonlinear least-square parameter minimization to determine the best-fit values with the corrections for the tight-binding inhibition; i.e., the data was transferred into the software KaleidaGraph and fitted by the aforementioned equations.

In addition, the resulting inhibition constants and rate constants were found to be consistent with those obtained under the condition of high substrate concentration where the inhibitor concentrations were at least 10-fold greater than the enzyme concentration (i.e., $[I]_t >> [E]_t$). K_i and K_i^* were estimated by fitting initial rates (V_0) and final steady-state rates (V_S) against inhibitor concentrations and using the equations as follows: $V_0 = V_{max}\,[S]/(K_m\,(1 + [I]/K_i) + [S])$ and $V_S = V_{max}\,[S]/(K_m\,(1 + [I]/K_i^*) + [S])$.

The rate constant k_6, for the dissociation of the second enzyme-inhibitor complex can be also measured directly from the inhibitor release studies as described below.

Dissociation of E·I* Complex

The E·I* complex of the α-fucosidase and inhibitor (**2, 3, 4,** or **5**) was prepared by incubation of 10 μM α-fucosidase with different concentrations of inhibitor (125 and 150 μM) at 20°C for 60 min. An aliquot of the incubation mixture was withdrawn and diluted 10^5-fold in 200 μl of 50 mM HEPES buffer (pH 8.0) containing 100 μM 4-methylumbelliferyl-α-L-fucopyranoside as the assay substrate. Recovery of the enzyme activity was measured by monitoring the emission at 465 nm based on an excitation wavelength of 360 nm. The resulting data was transferred into the software KaleidaGraph and fitted by equation 2 to determine the dissociation constant k_6 and $t_{1/2}$ (half-life of the E·I* complex).

Fluorescence Analysis of the Enzyme-Inhibitor Complex

The change of α-fucosidase intrinsic fluorescence upon the addition of compound **3** was monitored using an F-4500 fluorescence spectrometer (Hitachi Co., Japan). The emission spectra were recorded from 300 to 450 nm upon the excitation of α-fucosidase at 285 nm. The fluorescence spectra of 0.44 μM α-fucosidase in 50 mM HEPES buffer (pH 8.0) at 20°C were measured before and after addition of compound **3** (Figure 6A). The fluorescence changes ($F - F_0$) were plotted against the inhibitor concentration at the emission wavelength of 336 nm (Figure 6B).

The rate constants (k_{obs}) for the time-dependent increase in intrinsic fluorescence at each inhibitor concentration were calculated by computer fitting of the data to a first-order equation of the form, $y = a + b\,\exp(-k_{obs})$ using the software KaleidaGraph. These k_{obs} values were then fitted to the equation $k_{obs} = k_5\,[I]/(K_i + [I])$ to give computer-calculated values of K_i and k_5.

Supplemental Data

^{1}H NMR spectra of compounds **2–5** are available online at http://www.chembiol.com/cgi/content/full/11/9/1301/DC1.

Acknowledgments

This work was supported by National Science Council (NSC 92-2113-M-001-024 & NSC 92-2113-M-001-065 to C.H.L.) and Academia Sinica, Taiwan.

Received: April 27, 2004
Revised: June 27, 2004
Accepted: July 14, 2004
Published: September 17, 2004

References

1. Sels, J.P., Huijberts, M.S., and Wolffenbuttel, B.H. (1999). Miglitol, a new α-glucosidase inhibitor. Expert Opin. Pharmacother. *1*, 149–156.
2. Scott, L.J., and Spencer, C.M. (2000). Miglitol: a review of its therapeutic potential in type 2 diabetes mellitus. Drugs *59*, 521–549.
3. Asano, N. (2003). Glycosidase inhibitors: update and perspectives on practical use. Glycobiology *13*, 93R–104R.
4. Goss, P.E., Baker, M.A., Carver, J.P., and Dennis, J.W. (1995). Inhibitors of carbohydrate processing: a new class of anticancer agents. Clin. Cancer Res. *1*, 935–944.
5. Parish, C.R., Freeman, C., and Hulett, M.D. (2001). Heparanase: a key enzyme involved in cell invasion. Biochim. Biophys. Acta *1471*, M99–M108.
6. Roth, J., Zuber, C., Guhl, B., Fan, J.Y., and Ziak, M. (2002). The importance of trimming reactions on asparagine-linked oligosaccharides for protein quality control. Histochem. Cell Biol. *117*, 159–169.
7. Herscovics, A. (1999). Importance of glycosidases in mamma-

lian glycoprotein biosynthesis. Biochim. Biophys. Acta *1473*, 96–107.

8. Misaizu, T., Matsuki, S., Strickland, T.W., Takeuchi, M., Kobata, A., and Takasaki, S. (1995). Role of antennary structure of N-linked sugar chains in renal handling of recombinant human erythropoietin. Blood *86*, 4097–4104.
9. Lew, W., Chen, X., and Kim, C.U. (2000). Discovery and development of GS 4104 (oseltamivir): an orally active influenza neuraminidase inhibitor. Curr. Med. Chem. *7*, 663–672.
10. Mitrakou, A., Tountas, N., Raptis, A.E., Bauer, R.J., Schulz, H., and Raptis, S.A. (1998). Long-term effectiveness of a new α-glucosidase inhibitor (BAY m1099-miglitol) in insulin-treated type 2 diabetes mellitus. Diabet. Med. *15*, 657–660.
11. Moloney, D.J., Shair, L.H., Lu, F.M., Xia, J., Locke, R., Matta, K.L., and Haltiwanger, R.S. (2000). Mammalian Notch1 is modified with two unusual forms of O-linked glycosylation found on epidermal growth factor-like modules. J. Biol. Chem. *275*, 9604–9611.
12. Hooper, L.V., and Gordon, J.I. (2001). Glycans as legislators of host-microbial interactions: spanning the spectrum from symbiosis to pathogenicity. Glycobiology *11*, 1R–10R.
13. Hiraishi, K., Suzuki, K., Hakomori, S., and Adachi, M. (1993). Le(y) antigen expression is correlated with apoptosis (programmed cell death). Glycobiology *3*, 381–390.
14. Sulzenbacher, G., Bignon, C., Nishimura, T., Tarling, C.A., Withers, S.G., Henrissat, B., and Bourne, Y. (2004). Crystal structure of Thermotoga maritima α-L-fucosidase. Insights into the catalytic mechanism and the molecular basis for fucosidosis. J. Biol. Chem. *279*, 13119–13128.
15. Tarling, C.A., He, S., Sulzenbacher, G., Bignon, C., Bourne, Y., Henrissat, B., and Withers, S.G. (2003). Identification of the catalytic nucleophile of the family 29 α-L-fucosidase from Thermotoga maritima through trapping of a covalent glycosyl-enzyme intermediate and mutagenesis. J. Biol. Chem. *278*, 47394–47399.
16. Lowe, J.B. (2002). Glycosylation in the control of selectin counter-receptor structure and function. Immunol. Rev. *186*, 19–36.
17. Ayude, D., Fernandez-Rodriguez, J., Rodriguez-Berrocal, F.J., Martinez-Zorzano, V.S., de Carlos, A., Gil, E., and de La Cadena, M.P. (2000). Value of the serum α-L-fucosidase activity in the diagnosis of colorectal cancer. Oncology *59*, 310–316.
18. Fernandez-Rodriguez, J., Ayude, D., de La Cadena, M.P., Martinez-Zorzano, V.S., de Carlos, A., Caride-Castro, A., de Castro, G., and Rodriguez-Berrocal, F.J. (2000). α-L-fucosidase enzyme in the prediction of colorectal cancer patients at high risk of tumor recurrence. Cancer Detect. Prev. *24*, 143–149.
19. Glick, M.C., Kothari, V.A., Liu, A., Stoykova, L.I., and Scanlin, T.F. (2001). Activity of fucosyltransferases and altered glycosylation in cystic fibrosis airway epithelial cells. Biochimie *83*, 743–747.
20. Scanlin, T.F., and Glick, M.C. (1999). Terminal glycosylation in cystic fibrosis. Biochim. Biophys. Acta *1455*, 241–253.
21. Giardina, M.G., Matarazzo, M., Morante, R., Lucariello, A., Varriale, A., Guardasole, V., and De Marco, G. (1998). Serum α-L-fucosidase activity and early detection of hepatocellular carcinoma: a prospective study of patients with cirrhosis. Cancer *83*, 2468–2474.
22. Wu, C.-Y., Chang, C.-F., Chen, J.S.-Y., Wong, C.-H., and Lin, C.-H. (2003). Rapid diversity-oriented synthesis followed by in situ screening: identification as potent and selective α-fucosidase inhibitors. Angew. Chem. Int. Ed. Engl. *42*, 4661–4664.
23. Morrison, J.F., and Walsh, C.T. (1988). The behavior and significance of slow-binding enzyme inhibitors. Adv. Enzymol. Relat. Areas Mol. Biol. *61*, 201–301.
24. Lin, C.-H., Chen, S., Kwon, D.S., Coward, J.K., and Walsh, C.T. (1997). Aldehyde and phosphinate analogs of glutathione and glutathionylspermidine: potent, selective binding inhibitors of the *E. coli* bifunctional glutathionylspermidine synthetase/amidase. Chem. Biol. *4*, 859–866.
25. Matagne, A., Ghuysen, M.F., and Frere, J.M. (1993). Interactions between active-site-serine β-lactamases and mechanism-based inactivators: a kinetic study and an overview. Biochem. J. *295*, 705–711.
26. Becker, R.A., and Scholkens, B. (1987). Ramipril: review of pharmacology. Am. J. Cardiol. *59*, 3D–11D.
27. Goli, U.B., and Galardy, R.E. (1986). Kinetics of slow, tight-binding inhibitors of angiotensin converting enzyme. Biochemistry *25*, 7136–7142.
28. Houtzager, V., Ouellet, M., Falgueyret, J.P., Passmore, L.A., Bayly, C., and Perciival, M.D. (1996). Inhibitor-induced changes in the intrinsic fluorescence of human cyclooxygenase-2. Biochemistry *35*, 10974–10984.
29. Pandhare, J., Dash, C., Rao, M., and Deshpande, V. (2003). Slow tight-binding inhibition of proteinase K by a proteinaceous inhibitor: conformational alterations responsible for conferring irreversibility to the enzyme-inhibitor complex. J. Biol. Chem. *278*, 48735–48744.
30. Dash, C., Vathipadiekal, V., George, S.P., and Rao M. (2002). Slow tight-binding inhibition of xylanase by an aspartic protease inhibitor: kinetic parameters and conformational changes that determine the affinity and selectivity of the bifunctional nature of the inhibitor. J. Biol. Chem. *277*, 17978–17986.
31. Legler, G. (1990). Glycoside hydrolases: mechanistic information from studies with reversible and irreversible inhibitors. In Advances in Carbohydrate Chemistry and Biochemistry, R.S. Tipson and D. Horton, eds. (San Diego: Academic Press). pp. 319–384.
32. Lohse, A., Hardlei, T., Jensen, A., Plesner, I.W., and Bols, M. (2000). Investigation of the slow inhibition of almond β-glucosidase and yeast isomaltase by 1-azasugar inhibitors: evidence for the 'direct binding' model. Biochem. J. *349*, 211–215.
33. Bulow, A., Plesner, I.W., and Bols, M. (2000). A large difference in the thermodynamics of binding of isofagomine and 1-deoxynojirimycin to β-glucosidase. J. Am. Chem. Soc. *122*, 8567–8568.
34. Schramm, V.L. (2003). Enzymatic transition state poise and transition state analogs. Acc. Chem. Res. *36*, 588–596.
35. Lewandowicz, A., Tyler, P.C., Evans, G.B., Furneaux, R.H., and Schramm, V.L. (2003). Achieving the ultimate physiological goal in transition state analogue inhibitors for purine nucleoside phosphorylase. J. Biol. Chem. *278*, 31465–31468.
36. Fedorov, A., Shi, W., Kicska, G., Fedorov, E., Tyler, P.C., Furneaux, R.H., Hanson, J.C., Gainsford, G.J., Larese, J.Z., Schramm, V.L., et al. (2001). Transition state structure of purine nucleoside phosphorylase and principles of atomic motion in enzymatic catalysis. Biochemistry *40*, 853–860.
37. Ponasik, J.A., Strickland, C., Faerman, C., Savvides, S., Karplus, P.A., and Ganem B. (1995). Kukoamine A and other hydrophobic acylpolyamines: potent and selective inhibitors of Crithidia fasciculata trypanothione reductase. Biochem. J. *311*, 371–375.
38. Faerman, C.H., Savvides, S.N., Strickland, C., Breidenbach, M.A., Ponasik, J.A., Ganem, B., Ripoll, D., Krauth-Siegel, R.L., and Karplus, P.A. (1996). Charge is the major discriminating factor for glutathione reductase versus trypanothione reductase inhibitors. Bioorg. Med. Chem. *4*, 1247–1253.